Published in final edited form as:
Radiat Res. 2010 January ; 173(1): 10–20. doi:10.1667/RR1911.1.

Revisiting Strain-Related Differences in Radiation Sensitivity of the Mouse Lung: Recognizing and Avoiding the Confounding Effects of Pleural Effusions

Isabel L. Jackson[a], **Zeljko Vujaskovic**[a], and **Julian D. Down**[b,1]

[a]Department of Radiation Oncology, Duke University Medical Center, Durham, North Carolina

[b]Harvard–Massachusetts Institute of Technology Division of Health Sciences and Technology, Massachusetts Institute of Technology, Cambridge, Massachusetts

Abstract

The mouse has been used extensively to model radiation injury to the lung, a major dose-limiting organ for radiotherapy. Substantial differences in the timing and sensitivity of this tissue between mouse strains have been reported, with some strains, including C57BL/6, being designated as "fibrosis-prone". Pleural effusions have also been reported to be a prominent problem in many mouse strains, but it remains unclear how this affects the lung function and survival of the standard C57BL/6 mouse. The purpose of this investigation was to re-evaluate this strain in comparison with C57L and CBA mice after whole-thorax irradiation at doses ranging from 10 to 15 Gy. Breathing rate measurements, micro-computerized tomography, lung tissue weight, pleural fluid weight and histopathology showed that the most prominent features were an early phase of pneumonitis (C57L and CBA) followed by a late incidence of massive pleural effusions (CBA and C57BL/6). A remarkable difference was seen between the C57 strains: The C57L mice were exquisitely sensitive to early pneumonitis at 3 to 4 months while C57BL/6 mice showed a delayed response, with most mice presenting with large accumulations of pleural fluid at 6 to 9 months. These results therefore caution against the routine use of C57BL/6 mice in radiation lung experiments because pleural effusions are rarely observed in patients as a consequence of radiotherapy. Future experiments designed to investigate genetic determinants of radiation lung damage should focus on the high sensitivity of the C57L strain (in comparison with CBA or C3H mice) and the possibility that they are more susceptible to pulmonary fibrosis as well as pneumonitis.

INTRODUCTION

Radiation damage to pulmonary tissue is often described as either an inflammatory pneumonitis reaction or chronic fibrosis characterized by collagen accumulation (1). The relative importance of these two pathologies in humans is dependent upon the volume of lung irradiated as well as the accumulated radiation dose. The pneumonitis reaction, sometimes referred to as pneumonopathy or alveolitis, has a characteristic latent period with an acute onset within the first 6 months after treatment. It becomes life-threatening when the entire lung tissue is exposed to wide-field radiotherapy or after radiation accidents, ranking this organ one of the most radiosensitive after the hematopoietic system (2–6). Radiation pulmonary fibrosis is usually asymptomatic and becomes a concern only at later times and at higher radiation doses limited

[1]Address for correspondence: Harvard-MIT Health Sciences and Technology, Bldg. E25-406, Massachusetts Institute of Technology, 45 Carleton Street, Cambridge, MA 02142; jddown@mit.edu.

to a portion of the lung (1,7–9). It is also well acknowledged that intrinsic variability among patients plays a significant role, and this has encouraged an active preclinical research program to explore genetic factors that determine the severity of radiation lung damage (10). Diverse responses among different genetic strains of mice receiving thoracic irradiation have been recognized and provide an opportunity to identify the critical molecular mechanisms that determine lung damage. Strain differences were first described for CBA mice, which typically displayed two phases of lung dysfunction and mortality associated with early pneumonitis and late pleural effusions, and for C57BL/Cbi mice, which exhibited no discernable pneumonitis that affected survival but were equally sensitive to the later phase (11). Other studies showed that the timing of these two pathologies can vary independently among rodents, with C3H mice exhibiting responses similar to CBA mice (12) and WHT, TO, BALB/cJ and SWR/J mice as well as August and Wistar rats exhibiting a mixture of early pleural effusions and pneumonitis (13–16). A steep radiation dose-dependent rise in pleural fluid levels during the late phase has been demonstrated that, under conditions of dose modification by the radioprotector amifostine (WR2721) and continuous low dose rate, follows the concurrent assessment of breathing rate and lethality (17,18). Pulmonary fibrosis quantified by hydroxyproline measurements, however, does not follow these other end points during the late phase (17,19) and therefore appears to play a minimal role and may be a residual consequence of the preceding pneumonitis reaction. Franko and colleagues investigated histopathological sequelae of whole-thorax irradiation in a number of different mouse strains and broadly categorized C57 mouse strains (C57L/J, C57BL/6J and C57BL/10J) as being “fibrosis-prone” through the observation of focal fibrotic lesions in the lungs (14,20,21). While pleural effusions were also reported in 15 of 17 mouse strains studied, the histological appearance of fibrosis dominated the interpretation of the results. The C57BL/6 mouse was adopted in further studies as a strain that is presumed to be susceptible to the lethal effects of pulmonary fibrosis after whole-thorax irradiation. The C57BL/6 mouse is also the most widely used strain in biomedical studies and is the background of choice for creating lines with various genetic modifications. This, however, should not pre-empt their consideration as a model of radiation lung damage that can be related to the human condition.

The present work employed this same mouse substrain to show that they exhibit a late response dominated by a large accumulation of pleural fluid, similar to CBA mice, and in accordance with previous findings in C57BL/Cbi mice. The C57L mouse strain, however, proved to be very different in exhibiting a high sensitivity toward early pulmonary injury after whole-thorax irradiation and should be considered as an alternative model for further investigations of the genetic predisposition toward radiation lung damage.

MATERIALS AND METHODS

Male C57BL/6, CBA and C57L mice were housed under similar conditions in facilities at either the University Medical Center Groningen (UMCG) or the Massachusetts Institute of Technology (MIT). The C57BL/6 and CBA mice were obtained from either Iffacredo, L’Arbresle, France (C57BL/6JIco and CBA/JIco used at UMCG) or Jackson Laboratory, Bar Harbor, ME (C57BL/6J and CBA/J used at MIT), while all C57L/J mice were from Jackson Laboratory (UMCG and MIT). Both facilities were free of known pathogenic organisms (Sendai, MHV, PVM, GD VII, REO 111, EMC, LMC, MVM, K. and M. pulmonis). Experiments at UMCG were performed in accordance with the Netherlands Experiments on Animals Act (1977) and the European Convention for the protection of vertebrate animals used for experimental purposes (Strassbourg, 18.111.1986), and experiments at MIT were approved by the Institutional Animal Care and Use Committee. At the UMCG, groups of four mice (16 weeks of age) were irradiated simultaneously with 10, 12.5 or 15 Gy of 200 kVp X rays (Mueller MG 300, Philips, Eindhoven, The Netherlands, HVL = 1.05 mm copper, dose rate = 0.44 Gy min^{-1}) delivered to the thorax through 21-mm-long apertures with 3 mm lead shielding

of the head and abdomen. At MIT, the thoraces of mice (12 weeks of age) were irradiated individually at the same doses using ^{137}Cs γ rays (GammaCell 40, Atomic Energy Limited, Ottawa, Canada) at a dose rate of 0.51 Gy min^{-1} through a 25-mm-long aperture with 28 mm lead shielding of the head and abdomen. These dose rates fall in the range for producing equivalent lung damage without radiation dose sparing (18). X-ray dosimetry was performed using a calibrated ionization chamber, and γ-ray dosimetry was determined using calibrated LiF thermoluminescence dosimeters (Radiation Dosimetry Services, The University of Texas M. D. Anderson Cancer Center, Houston, TX) placed in tissue-equivalent material. The mice were irradiated without anesthesia and were contained within holders as described previously (22). All experiments included sham-irradiated controls.

Pulmonary function was assessed from the resting breathing rates measured in a 160-ml total-body plethysmograph as described by Travis *et al.* (23). The physical condition of the mice was monitored closely and the mice were euthanized by CO_2 asphyxiation when they entered respiratory distress and their rectal temperature fell below 34°C. The thorax was opened carefully to avoid bleeding and the pleural fluid was absorbed onto preweighed tissue paper and weighed again. The lungs were then excised, removing trachea and bronchial structures, washed in cold phosphate-buffered saline, blotted and weighed. The left lobe was inflated through the left bronchus with 10% neutral buffered formalin. After fixation it was embedded in paraffin; 4-μm sections were cut and stained with Masson's trichrome.

X-ray microcomputerized tomography (micro-CT) was performed on mice under isoflurane (1–2% with oxygen) anesthesia using an eXplore Locus Micro CT Scanner with MicroView 2.1. software (GE Medical Systems, London, ON, Canada). CT images were acquired with the X-ray source biased at 80 kVp and 450 μA with 400 projections, exposure time of 400 ms, detector bin mode of 2 × 2, and an effective pixel size of 0.047 mm. The total scan time was about 14 min with real-time reconstruction. High-resolution reconstruction of the images was performed and volumetric analysis was performed from three-dimensional images of the lung created by isosurface profiling within a defined region of interest (ROI). Threshold voxels of between −213 and −282 Hounsfield units (HU) for the control mice and between −87 and −244 HU for the irradiated mice were required to obtain reasonable three-dimensional images that defined the lung surface; the threshold at higher HU for some of the irradiated mice was attributed to the increase in lung density. The tracheal-bronchial tree outside the lung was delineated similarly and subtracted from the lung volume. Lung parenchyma density measurements were obtained from the average HU within cylindrical ROIs (1.0 mm diameter, 1.0 mm length) that were positioned within the left and right lung and avoided both high-density large blood vessels and the motion artifacts at the lung boundary.

Magnetic resonance imaging (MRI) was performed, also under isoflurane anesthesia, using a 4.7-Tesla MRI machine (Bruker BioSpin Corporation, Billerica, MA) with a mouse body coil. T2 weighted images (coronal and axial) were taken with eight averages, repetition time of 2000 ms (2508.37 ms for axial view), echo time of 12 ms (effective echo time is 36.0 ms), and matrix size of 192 × 192 × 16 (coronal view) or 192 × 192 × 24 (axial view) with voxels of 0.288 mm × 0.208 mm × 1.0 mm, respectively. Images were acquired using Paravision 4.0 software (Bruker BioSpin Corporation).

RESULTS

A comparison of survival times for each mouse strain and radiation dose treated at UMCG with 200 kVp X rays or at MIT with ^{137}Cs γ rays is provided in Table 1. The major distinctions were in the prolongation of survival of C57BL/6 mice compared to CBA mice at the highest dose of 15 Gy and the lower overall tolerance of C57L/J mice. There were relatively minor differences among treatment groups coming from the two institutions with the exception of

C57L/J mice given 10 Gy whole-thorax irradiation at UMGC that proved to be lethal at about 17 weeks after orthovoltage X irradiation while the mice given γ radiation at MIT survived to 28 weeks without signs of respiratory distress.

The time course for resting breathing frequency (expressed as a ratio of the unirradiated controls) and percentage survival for each radiation dose group is shown in Fig. 1. CBA/JIco mice that received either 12.5 or 15 Gy X radiation showed a progressive increase in breathing rate after 8 weeks, with the higher dose producing a maximal mean value at 14 weeks followed by a rapid decrease in survival. The dose of 12.5 Gy produced smaller increases in breathing rate over this period; the mice continued to hyperventilate out to 33 weeks, with loss of two mice at 26 and 30 weeks (Fig. 1A). C57BL/6JIco mice showed a more progressive response, with the high-dose group preceding the low-dose group. The highest breathing rates were reached at 27 weeks, coincident with mortality (Fig. 1B). In contrast, C57L/J mice exhibited a very rapid onset of tachyapnea and mortality, even at the lowest dose of 10 Gy. No C57L/J mice survived beyond 18 weeks (Fig. 1C).

Figure 2A displays the fresh lung mass of individual CBA, C57BL/6 and C57L mice as a function of the time at which they were euthanized with respiratory distress. Between 14 and 18 weeks after treatment, all mice euthanized were of the CBA or C57L strains and had lung weights in excess of 350 mg. This was always associated with visual reddening and consolidation of the tissue (hepatization). Surface scarring was an additional feature observed on lungs from three C57L/J mice at 17–18 weeks after 10 Gy. Most animals euthanized for respiratory distress beyond 35 weeks were of the C57BL/6 strain; 11 of 13 mice had lung weights below 350 mg. In contrast to CBA and C57L mice autopsied before 6 months, the majority of the C57BL/6 mice displayed either normal or multifocal reddening of the lungs and were not resistant to inflation with fixative. As shown in Fig. 2B, these differences in lung weight and morphology were conversely related to the amount of pleural fluid. There were only slight changes in fluid levels in the CBA and C57L mice that had the early increase in lung mass, while at later times most mice had large amounts of pleural fluid (11 of 13 C57BL/6 mice had levels of above 1.0 g).

Representative coronal and axial slices through the mid-thorax of the CT image volumes from a CBA/J control mouse and from irradiated CBA/J (15 Gy), C57L/J (12.5 Gy) and C57BL/6J (15 Gy) mice at 15–16 weeks in Fig. 3A show increased regions of radio-opacity within the lung parenchyma in irradiated CBA/J and C57L/J mice, while the lungs of C57BL/6J mice appeared normal at this time. Quantification of CT lung density from the average of left and right lung ROI showed a significant dose-dependent increase only in CBA/J and C57L/J mice (the latter occurring at lower radiation doses) (Fig. 4). The decrease in estimated lung volume at 15–16 weeks in some of the mice (with densities above −300 HU) was associated with exclusion of heterogeneous high-density regions from the isosurface profiles.

The remaining three C57L/J mice given 10 Gy γ radiation survived out to 28 weeks with no obvious signs of respiratory distress. Evaluation of lung CT at this time, however, revealed multi-focal radio-opaque lesions within the lungs (Fig. 3B) and moderate increases in tissue density (Fig. 4).

CT images and analysis of irradiated C57BL/6J mice at the later time of 28–30 weeks showed both an increase in lung density and a decrease in lung volume that appeared to be related to the amount of pleural fluid in those mice that were autopsied on the day of CT imaging (Fig. 3C and Fig. 4). The presence of pleural effusion was more clearly distinguished above the diaphragm on T2-weighted MRI images (Fig. 3C). Notably, this was observed at a moderate level of pleural fluid (0.3 ml) that did not produce respiratory distress but is still expected to cause a significant elevation in breathing frequency (17,18).

Histological sections of lung tissues from two CBA/J mice experiencing respiratory distress at 18 weeks after 15 Gy whole-thorax irradiation were reviewed and showed extensive injury to most of the parenchyma typical of pneumonitis (alveolitis) with the features of abundant alveolar macrophages, heavy mononuclear infiltrates of the septa and interstitial and intra-alveolar edema and lymphocytic perivascular cuffing (Fig. 5B) as described previously for this mouse strain (14,24). Analysis of one CBA/J mouse given a lower dose of 12.5 Gy at 34 weeks with a pleural effusion showed lungs with a relative normal pathology with the exception of occasional areas of foamy macrophages (Fig. 5C).

Histological sections of four C57L/J mice all showed similar extensive pneumonitis throughout the lungs during the early phase but at the lower dose of 12.5 Gy (Fig. 5D). Focal areas of blue staining indicative of initiation of fibrosis were also noted in this strain (Fig. 5E) but were minimal compared to the magnitude of pneumonitis. The marked reduction of aerated lung from the increased inflammatory cellularity and edema explains both the increase in lung mass (Fig. 2) and CT lung density (Figs. 3 and 4) observed for CBA/J and C57L/J mice during the pneumonitic phase.

The three surviving C57L/J mice receiving 10 Gy whole-thorax irradiation and terminated at 28 weeks exhibited multiple gray lesions with dimpled appearance of the lung surface on autopsy. The lung tissues, however, were not reddened, firm or resistant to expansion with fixative in contrast to the sick C57L/J mice autopsied earlier at 14–18 weeks. The lung tissue weights were moderately increased (298, 303 and 345 mg) as compared to the one control C57L/J mouse (195 mg), and there was no incidence of pleural effusions (less than 0.1 ml). Microscopic examination of these lungs revealed abundant alveolar macrophages throughout the tissues and discrete multifocal lesions of dense collagen accumulation accompanied by alveolar collapse in all three of the mice irradiated with 10 Gy. Most of these lesions were subpleural, extending internally and associated with distortion of the lung surface (Fig. 5F) to account for the dimpled appearance observed macroscopically. The presence of elongated crystalline material lodged in the terminal bronchioles and alveolar ducts were also characteristic in areas of fibrosis. The pathology of multifocal dense regions of fibrosis is in keeping with the radio-opaque lesions observed on micro-CT (Fig. 3B) and was more overt than that observed in C57BL/6 mice during the late phase.

Histological sections from seven C57BL/6J mice at 28 to 32 weeks after 15 Gy irradiation exhibited variable levels of microscopic injury that appeared to be more extensive for those animals with the higher lung weights; in many of the mice the changes were relatively minor (Fig. 5G), while in one mouse the pneumonitis appeared quite severe (Fig. 5I). The large variations in degree of lung damage may be attributed to the intrusion of pleural effusion that limited the survival of these mice and therefore prevented the full expression of concurrent lung injury. Very occasional focal areas of fibrosis were also evident, mostly localized to the sub-pleura (Fig. 5H), as documented previously in this strain during the late phase (20,25). Collagen staining was not as dense or extensive compared to C57L/J mice at 28 weeks after the much lower dose of 10 Gy as noted above.

DISCUSSION

The inclusion in the present study of mice belonging to the CBA strain provided a useful basis of comparison because these animals have been the most widely reported in displaying two phases of response after whole-thorax irradiation. This was first described by Travis and coworkers as being attributed to an early phase of pneumonitis followed by late fibrosis (24). This strain, along with C3H mice, has since been considered to produce a mild or non-existent fibrotic reaction in the lungs (20,25), leaving pleural effusions as the major culprit in producing both increased breathing rate and mortality beyond 6 months (13). It is important to appreciate

how volumes exceeding 1 ml have an impact on lung physiology in mice since this takes up most of the thorax at the obvious expense of lung occupancy. By analogy this would be equivalent to 2–4 liters in adult humans on a per weight basis. Respiratory distress culminating as lethality is therefore likely to be a consequence of such an extreme condition. These accumulations of pleural fluid are not just a phenomenon in pre-terminal mice, because a clear dose-dependent rise in pleural fluid content was seen in healthy mice, producing dose responses that agree very well with corresponding curves obtained from concurrent measurements of breathing rates, even under conditions where the late phase has been dissociated from the preceding pneumonitis response (17,18). In contrast, hydroxyproline content used as a biochemical index of fibrosis shows a poor correlation with any of the above end points of late damage (17,19) and may be a benign result of radiation pneumonitis. Micro-CT analysis of live CBA/J mice in the current study shows how pneumonitis at 4 months after whole-thorax irradiation directly causes an increase in lung tissue density, as expected from the elevation in lung weights, most probably associated with the pathology of edema and inflammatory cell infiltrates. These findings are similar to earlier results on CBA/Ca mice using low-resolution CT scans but where a different picture emerged at 9 months in which pleural fluid accumulations cause both a reduction in lung volume and a corresponding increase in tissue density through lung compression (26).

The salient pathophysiological features of the C57BL/6 mouse were very similar to those reported previously for the C57BL/Cbi substrain (11) in that the breathing rate response was prolonged and most mice ultimately presented with large volumes of pleural fluid with near-normal lung tissue weights. It appears unlikely that this phenomenon in C57BL/6 mice is an isolated finding confined to a particular institution or source of radiation, because comparable results were observed using either X rays or γ rays at UMCG and MIT, respectively, and at dose rates that are sufficiently high to not allow dose modification of lung damage (18). The absence of a clear wave of deaths attributable to pneumonitis is also in keeping with the results of Down and Steel (11) and Sharplin and Franko (20). In the former study, all 13 C57BL/Cbi mice in respiratory distress had pleural effusions on autopsy, while Sharplin and Franko (20) reported pleural effusion in one of four C57BL/6J mice during the late phase, but the levels of pleural fluid were not systematically measured in all mice that were autopsied and its role in impaired lung function may have been underestimated. Pleural effusion was present in all C57/BL10J mice (20) and in a majority (80%) of mice in which the C57BL/6J mice were crossed with other mouse strains (21). These authors placed emphasis on their findings of obstructed acini and concluded that lack of perfusion of apparently normal lung is a likely factor in respiratory insufficiency (20), a phenomenon that may be the consequence of atelectasis associated with pressure exerted on lung tissue from the surrounding accumulation of pleural fluid. A variable picture of pneumonitis was observed in our C57BL/6J mice experiencing respiratory distress, but in most cases this was relatively mild. In contrast to the histological appearance noted in C57BL/Cbi mice (11), focal areas of blue staining indicative of fibrosis were also observed; this is consistent with an average of only about 5% of the lung section area affected by this lesion as reported by Delito and Travis (25). In no case did we observe extensive contracted fibrosis.

The development of tachypnea at 6 months and beyond after irradiation of C57BL/6JIco mice is again in accordance with restricted breathing from the accumulation of pleural fluid as observed on X-ray CT scans in C57BL/Cbi mice (26). The compression atelectasis and reduced *in situ* pulmonary compliance from the external effects of pleural effusion also explains the increased radiological density and decreased lung volumes in most of the C57BL/6J mice receiving 15 Gy as shown from micro-CT, with pleural fluid accumulation visualized more definitively in T2-weighted MRI. It is notable that elevated *in situ* lung tissue density and/or reduced lung volume has been similarly documented in this strain and period (27,28), but the

present results raise questions about the previous assertion that such radiological changes are attributed solely to pulmonary fibrosis.

Radiation-induced pleural effusions were first observed in whole-body-irradiated and bone marrow-transplant rescued mice (29–31) at radiation doses and latent times that would be predicted from an extrapolation of the direct effect of thoracic irradiation. Gross (32) was the first to describe the high incidence of pleural effusions after whole-thorax irradiation in CF1 mice; this phenomenon has now been documented in a number of other mouse strains (11–14,20,21) as well as different strains of rats (15,16,33–36). In some mouse strains and in rats, pleural effusion can arise early, either preceding or interfering with the expression of radiation pneumonitis (13). Thus the timing of these two independent pathologies varies widely among different rodent strains, as illustrated in Fig. 6. In spite of these numerous earlier reports of pleural effusions emanating from different laboratories and including C57BL mice, this strain, or the various genetic modifications thereof, is being used increasingly in long-term studies without documentation of the presence or absence of effusions (*e.g.* 27,39–41). It therefore remains uncertain that the respiratory insufficiency and/or mortality after whole-thorax irradiation in these studies are the direct result of pulmonary fibrosis. Some recent reports document reduced fibrosis according to either histological or biochemical criteria in C57BL/6 mice genetically deficient in ICAM-1 (42) or integrin αvβ6 (43) or treated with antioxidant enzymes (44), but this has not translated into improved animal survival. Further evidence for a lack of correlation between pulmonary fibrosis and mortality comes from the similarity in tolerance of “fibrosis-resistant” CBA and “fibrosis-prone” C57BL strains during the late phase.

Despite the similarity in the strain nomination, our parallel investigation of the C57L/J mouse strain revealed a response that contrasted considerably from the C57BL/6 model. In this case all mice receiving 12.5 as well as 15 Gy succumbed to the lethal effects of early pneumonitis with no evidence of pleural effusions. Orthovoltage X rays (10 Gy) also proved to be lethal for pneumonitis, while C57L/J mice given the same dose of ^{137}Cs γ radiation survived to at least 28 weeks. This dose appears to be critical in being close to the $LD_{50/180}$ of 11 Gy X rays as reported previously for this mouse strain (14). In the present study, the higher survival after 10 Gy γ irradiation may well be attributed to the slightly lower RBE of ^{137}Cs γ rays. The latter mice, however, still showed an increase in CT lung density at 4 months that increased further when the dose was increased to 12.5 Gy, comparable to the effects of increasing the dose from 12.5 to 15 Gy in CBA/J mice. The preceding and rapid rise in breathing rate between 12 to 16 weeks after 10–15 Gy mirrors the decrease in carbon monoxide uptake in this same strain and dose range as reported previously by Franko and Sharplin (45). It is of interest that our microscopic observations at both early and late times after whole-thorax irradiation indicate that pneumonitis in C57L/J mice may progress rapidly into fibrosis, as described previously (14,45). Indeed, this appeared to be quite extensive at later times after irradiation (45), with CT dense lesions remaining within the lungs at 28 weeks (Fig. 3B), and may account for persistent lung dysfunction observed in this strain (45), albeit without the high incidence of late lethality as seen in other C57 strains.

In conclusion, the early and exclusive incidence of radiation pneumonitis is observed only for CBA, C3H and C57L mice (Fig. 6), and hence these strains appear to be the most appropriate for studying the counterpart in humans. It should also be considered that the absence of a prominent fibrotic pathology in the lungs of CBA and C3H mice after exposure of the entire lung tissue is also representative of the clinical experience where the radiation doses at which widespread pneumonitis can be tolerated acceptably are usually at or below the lower limits of fibrosis (2,3,5,38). While the etiology of pleural effusions remains to be fully resolved, it can occur in the absence of direct damage to the lung, and investigators should appreciate that other tissues besides the lung can be injured by exposure of the whole thorax to radiation. The protein and albumen content of the effusates are consistent with an exudate (18) and bears a

resemblance to the occasional case reports of chylothorax that develop many years after clinical radiotherapy as a result of mediastinal fibrosis and occlusion of thoracic lymph vessels (46–48). In addition, radiation may be a contributing factor in exacerbating both pleural and pericardial effusions where surgical procedures such as esophagectomy may disrupt lymphatic channels that invest the region (49). Nonetheless, the incidence of pleural effusions is still rare as a side effect of radiotherapy alone. Thus the high frequency of pleural fluid accumulations in C57BL/6 mice after whole-thorax irradiation negates its usefulness as being fibrosis-prone and renders this strain among the most problematic to model radiation lung damage. C57L mice, on the other hand, appear to be a particularly interesting and promising model of radiation hypersensitivity confined to the lung with evidence for a more prominent evolution of fibrosis as well as pneumonitis. Further studies on radiation-induced lung pathology may also benefit by localizing the radiation to one lung, which enables higher doses to be delivered without the confounding problems of effusions or lethality while bringing the mouse closer to contoured radiotherapy of the thorax as encountered in the clinic.

Acknowledgments

The authors wish to thank Gregory Wojtkiewicz, Center for Molecular Imaging, Massachusetts General Hospital, Boston, MA, for performing the magnetic resonance imaging. This work was partially supported by NIH grant 5U19AI067798 and 5R01CA098452-04.

REFERENCES

1. Gross NJ. Pulmonary effects of radiation therapy. Ann. Intern. Med 1977;86:81–92. [PubMed: 319723]
2. Salazar OM, Rubin P, Keller B, Scarantino C. Systemic (half-body) radiation therapy: response and toxicity. Int. J. Radiat. Oncol. Biol. Phys 1978;4:937–950. [PubMed: 82551]
3. Van Dyk J, Keane TJ, Kan S, Rider WD, Fryer CJ. Radiation pneumonitis following large single dose irradiation: a re-evaluation based on absolute dose to lung. Int. J. Radiat. Oncol. Biol. Phys 1981;7:461–467. [PubMed: 7251416]
4. Keane TJ, Van Dyk J, Rider WD. Idiopathic interstitial pneumonia following bone marrow transplantation: the relationship with total body irradiation. Int. J. Radiat. Oncol. Biol. Phys 1981;7:1365–1370. [PubMed: 7033190]
5. Sampath S, Schultheiss TE, Wong J. Dose response and factors related to interstitial pneumonitis after bone marrow transplant. Int. J. Radiat. Oncol. Biol. Phys 2005;63:876–884. [PubMed: 16199317]
6. Baranov AE, Selidovkin GD, Butturini A, Gale RP. Hematopoietic recovery after 10-Gy acute total body radiation. Blood 1994;83:596–599. [PubMed: 8286754]
7. Rosen II, Fischer TA, Antolak JA, Starkschall G, Travis EL, Tucker SL, Hogstrom KR, Cox JD, Komaki R. Correlation between lung fibrosis and radiation therapy dose after concurrent radiation therapy and chemotherapy for limited small cell lung cancer. Radiology 2001;221:614–622. [PubMed: 11719654]
8. Choi YW, Munden RF, Erasmus JJ, Park KJ, Chung WK, Jeon SC, Park CK. Effects of radiation therapy on the lung: radiologic appearances and differential diagnosis. Radiographics 2004;24:985–997. [PubMed: 15256622]
9. Vågane R, Bruland OS, Fosså SD, Olsen DR. Radiological and functional assessment of radiation-induced pulmonary damage following breast irradiation. Acta. Oncol 2008;47:248–254. [PubMed: 18210300]
10. Travis EL. Genetic susceptibility to late normal tissue injury. Semin. Radiat. Oncol 2007;17:149–155. [PubMed: 17395045]
11. Down JD, Steel GG. The expression of early and late damage after thoracic irradiation: a comparison between CBA and C57Bl mice. Radiat. Res 1983;96:603–610. [PubMed: 6657925]
12. Down JD, Tarbell NJ, Warhol M, Mauch P. Dose-limiting complications from upper half body irradiation in C3H mice. Int. J. Radiat. Oncol. Biol. Phys 1988;14:483–489. [PubMed: 3277932]
13. Down JD. The nature and relevance of late lung pathology following localised irradiation of the thorax in mice and rats. Br. J. Cancer 1986;(Suppl. VII):330–332.

14. Sharplin J, Franko AJ. A quantitative histological study of strain-dependent differences in the effects of irradiation on mouse lung during the early phase. Radiat. Res 1989;119:1–14. [PubMed: 2756101]
15. Varekamp AE, de Vries AJ, Zurcher C, Hagenbeek A. Lung damage following bone marrow transplantation: II. The contribution of cyclophosphamide. Int. J. Radiat. Oncol. Biol. Phys 1987;13:1515–1521. [PubMed: 3305444]
16. van Rongen E, Tan CH, Durham SK. Late functional, biochemical and histological changes in the rat lung after fractionated irradiation to the whole thorax. Radiother. Oncol 1987;10:231–246. [PubMed: 3432599]
17. Down JD, Laurent GJ, McAnulty RJ, Steel GG. Oxygen-dependent protection of radiation lung damage in mice by WR 2721. Int. J. Radiat. Biol 1984;46:597–607.
18. Down JD, Easton DF, Steel GG. Repair in the mouse lung during low dose-rate irradiation. Radiother. Oncol 1986;6:29–42. [PubMed: 3520698]
19. Travis EL, Meistrich ML, Finch-Neimeyer MV, Watkins TL, Kiss I. Late functional and biochemical changes in mouse lung after irradiation: differential effects of WR-2721. Radiat. Res 1985;103:219–231. [PubMed: 2991972]
20. Sharplin J, Franko AJ. A quantitative histological study of strain-dependent differences in the effects of irradiation on mouse lung during the intermediate and late phases. Radiat. Res 1989;119:15–31. [PubMed: 2756106]
21. Franko AJ, Sharplin J, Ward WF, Hinz JM. The genetic basis of strain-dependent differences in the early phase of radiation injury in mouse lung. Radiat. Res 1991;126:349–356. [PubMed: 1852022]
22. Down JD, Collis CH, Jeffery PK, Steel GG. The effects of anesthetics and misonidazole on the development of radiation-induced lung damage in mice. Int. J. Radiat. Oncol. Biol. Phys 1983;9:221–226. [PubMed: 6833025]
23. Travis EL, Vojnovic B, Davies EE, Hirst DG. A plethysmographic method for measuring function in locally irradiated mouse lung. Br. J. Radiol 1979;52:67–74. [PubMed: 427355]
24. Travis EL, Down JD, Holmes SJ, Hobson B. Radiation pneumonitis and fibrosis in mouse lung assayed by respiratory frequency and histology. Radiat. Res 1980;84:133–143. [PubMed: 7454976]
25. Dileto CL, Travis EL. Fibroblast radiosensitivity *in vitro* and lung fibrosis *in vivo*: comparison between a fibrosis-prone and fibrosis-resistant mouse strain. Radiat. Res 1996;146:61–67. [PubMed: 8677299]
26. Nicholas D, Down JD. The assessment of early and late radiation injury to the mouse lung using X-ray computerised tomography. Radiother. Oncol 1985;4:253–263. [PubMed: 4081113]
27. Abdollahi A, Li M, Ping G, Plathow C, Domhan S, Kiessling F, Lee LB, McMahon G, Gröne HJ, Huber PE. Inhibition of platelet-derived growth factor signaling attenuates pulmonary fibrosis. J. Exp. Med 2005;201:925–935. [PubMed: 15781583]
28. Guerrero T, Castillo R, Noyola-Martinez J, Torres M, Zhou X, Guerra R, Cody D, Komaki R, Travis E. Reduction of pulmonary compliance found with high-resolution computed tomography in irradiated mice. Int. J. Radiat. Oncol. Biol. Phys 2007;67:879–887. [PubMed: 17293238]
29. Barnes DW, Bungay GT, Mole RH. Delayed mortality after mid-lethal exposures to whole body irradiation and its modification by treatment with syngeneic lymph-node or bone-marrow cells. Int. J. Radiat. Biol 1966;11:409–427.
30. Hollander CF, van Bekkum DW. Pathology of the late syndrome in mice lethally irradiated and treated with isologous bone-marrow transplantation. Int. J. Radiat. Biol 1969;16:70–71.
31. Covelli V, Metalli P, Briganti G, Bassani B, Silini G. Late somatic effects in syngeneic radiation chimaeras. II. Mortality and rate of specific diseases. Int. J. Radiat. Biol 1974;26:1–15.
32. Gross NJ. Experimental radiation pneumonitis: changes in physiology of the alveolar surface. J. Lab. Clin. Med 1978;92:991–1001. [PubMed: 739177]
33. Cardozo BL, Zoetelief H, van Bekkum DW, Zurcher C, Hagenbeek A. Lung damage following bone marrow transplantation: I. The contribution of irradiation. Int. J. Radiat. Oncol. Biol. Phys 1985;11:907–914. [PubMed: 3886609]
34. Ward WF, Molteni A, Ts'ao CH, Solliday NH. Pulmonary endothelial dysfunction induced by unilateral as compared to bilateral thoracic irradiation in rats. Radiat. Res 1987;111:101–106. [PubMed: 3037587]

35. Geraci JP, Jackson KL, Mariano MS, Michieli BM. Kidney and lung injury in irradiated rats protected from acute death by partial-body shielding. Radiat. Res 1990;122:95–100. [PubMed: 2108469]
36. Semenenko VA, Molthen RC, Li C, Morrow NV, Li R, Ghosh SN, Medhora MM, Li XA. Irradiation of varying volumes of rat lung to same mean lung dose: a little to a lot or a lot to a little? Int. J. Radiat. Oncol. Biol. Phys 2008;71:838–847. [PubMed: 18439765]
37. Down JD, Nicholas D, Steel GG. Lung damage after hemithoracic irradiation: dependence on mouse strain. Radiother. Oncol 1986;6:43–50. [PubMed: 3715060]
38. Fryer CJ, Fitzpatrick PJ, Rider WD, Poon P. Radiation pneumonitis: experience following a large single dose of radiation. Int. J. Radiat. Oncol. Biol. Phys 1978;4:931–936. [PubMed: 721655]
39. Rube CE, Uthe D, Schmid KW, Richter KD, Wessel J, Schuck A, Willich N, Rube C. Dose-dependent induction of transforming growth factor beta (TGF-beta) in the lung tissue of fibrosis-prone mice after thoracic irradiation. Int. J. Radiat. Oncol. Biol. Phys 2000;47:1033–1042. [PubMed: 10863076]
40. Epperly MW, Epstein CJ, Travis EL, Greenberger JS. Decreased pulmonary radiation resistance of manganese superoxide dismutase (MnSOD)-deficient mice is corrected by human manganese superoxide dismutase-plasmid/liposome (SOD2-PL) intratracheal gene therapy. Radiat. Res 2000;154:365–374. [PubMed: 11023599]
41. Chiang CS, Liu WC, Jung SM, Chen FH, Wu CR, McBride WH, Lee CC, Hong JH. Compartmental responses after thoracic irradiation of mice: strain differences. Int. J. Radiat. Oncol. Biol. Phys 2005;62:862–871. [PubMed: 15936571]
42. Hallahan DE, Geng L, Shyr Y. Effects of intercellular adhesion molecule 1 (ICAM-1) null mutation on radiation-induced pulmonary fibrosis and respiratory insufficiency in mice. J. Natl. Cancer Inst 2002;94:733–741. [PubMed: 12011223]
43. Puthawala K, Hadjiangelis N, Jacoby SC, Bayongan E, Zhao Z, Yang Z, Devitt ML, Horan GS, Weinreb PH, Munger JS. Inhibition of integrin αvβ6, an activator of latent TGFβ, prevents radiation-induced lung fibrosis. Am. J. Respir. Crit. Care Med 2008;177:82–90. [PubMed: 17916808]
44. Machtay M, Scherpereel A, Santiago J, Lee J, McDonough J, Kinniry P, Arguiri E, Shuvaev VV, Sun J, Christofidou-Solomidou M. Systemic polyethylene glycol-modified (PEGylated) superoxide dismutase and catalase mixture attenuates radiation pulmonary fibrosis in the C57BL/6 mouse. Radiother. Oncol 2006;81:196–205. [PubMed: 17069914]
45. Franko AJ, Sharplin J. Development of fibrosis after lung irradiation in relation to inflammation and lung function in a mouse strain prone to fibrosis. Radiat. Res 1994;140:347–355. [PubMed: 7972687]
46. Rodríguez-García JL, Fraile G, Moreno MA, Sánchez-Corral JA, Peñalver R. Recurrent massive pleural effusion as a late complication of radiotherapy in Hodgkin's disease. Chest 1991;100:1165–1166. [PubMed: 1914584]
47. Morrone N, Gama e Silva Volpe VL, Dourado AM, Mitre F, Coletta EN. Bilateral pleural effusion due to mediastinal fibrosis induced by radiotherapy. Chest 1993;104:1276–1278. [PubMed: 8404208]
48. van Renterghem DM, Pauwels RA. Chylothorax and pleural effusion as late complications of thoracic irradiation. Chest 1995;108:886–887. [PubMed: 7656656]
49. Murthy SC, Rozas MS, Adelstein DJ, Mason DP, Calhoun R, Rybicki LA, Feng J, Blackstone EH, Rice TW. Induction chemoradiotherapy increases pleural and pericardial complications after esophagectomy for cancer. J. Thorac. Oncol 2009;4:395–403. [PubMed: 19247086]

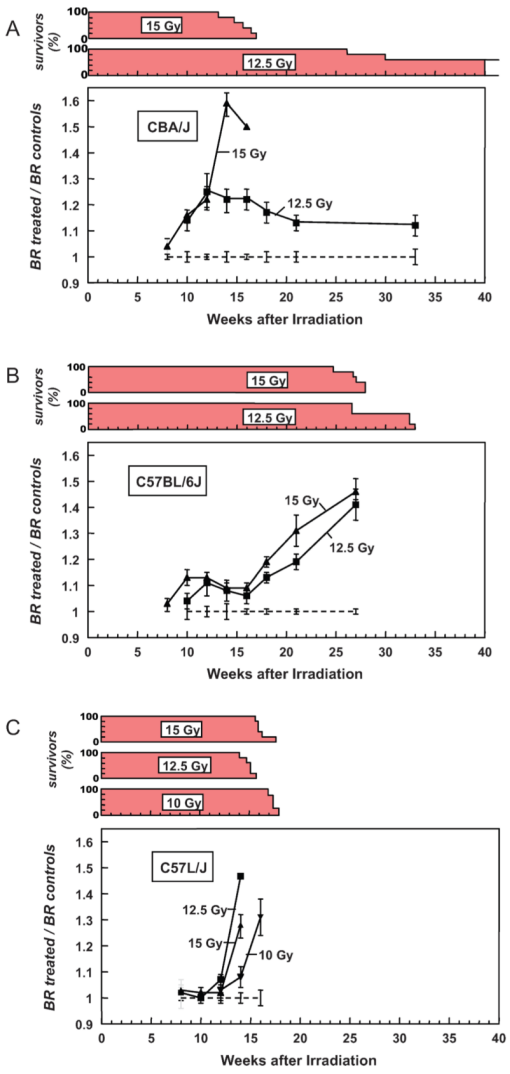

FIG. 1.

Breathing rate (BR), expressed as a ratio of controls, and percentage survival plotted as a function of time after single doses of whole-thorax irradiation (200 kVp X rays) to CBA/JIco (panel A), C57BL/6JIco (panel B) and C57L/J (panel C) mice. Each group consisted of five mice at the start. Error bars represent ±1 SEM.

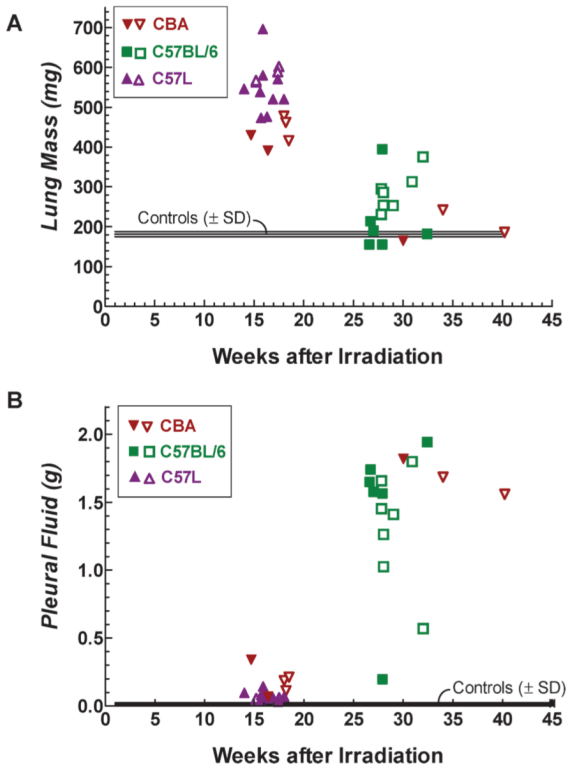

FIG. 2.

Fresh lung mass (panel A) and pleural fluid content (panel B) from individual CBA (▼, ▽), C57BL/6 (■, □) and C57L (▲, △) mice. Closed symbols are mice treated at UMCG (CBA/JIco, C57BL/6JIco and C57L/J) with 200 kVp X rays and open symbols are mice (CBA/J, C57BL/6J and C57L/J) treated at MIT with ^{137}Cs γ rays. All animals euthanized before 20 weeks showed severe gross damage (reddened and firm), while 14 of 16 mice euthanized at later times had lungs with moderate to no macroscopic changes but had massive pleural effusions. Shaded area represents the standard deviation (SD) around the mean of five unirradiated C57BL/6JIco control mice. Comparisons of the lung or pleural fluid weights using to the Mann-Whitney *U* test showed no difference ($P > 0.05$) between treatments with X rays (UMCG) and γ rays (MIT) for each strain (CBA or C57L mice at 14–18 weeks and C57BL/6 mice at 26–32 weeks).

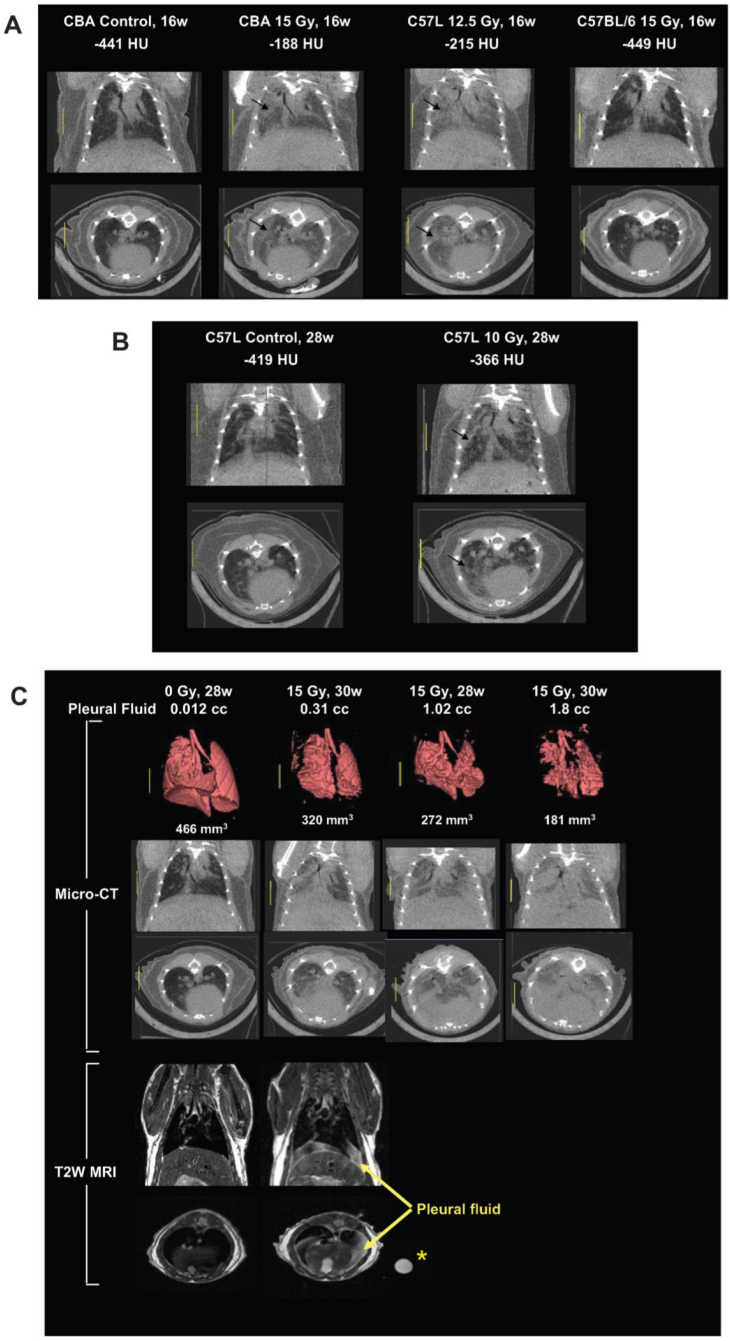

FIG. 3.

Panel A: Micro-CT coronal and axial sections through the mid-thorax of control and irradiated mice at 16 weeks after whole-thorax irradiation (^{137}Cs γ rays) to show regional increase in lung parenchyma density (arrows) associated with pneumonitis in treated CBA/J and C57L/J mice but not C57BL/6 mice. Panel B: Micro-CT sections of a control C57L/J mouse and a C57L/J mouse at 28 weeks after 10 Gy whole-thorax irradiation with focal radio-opaque lesions (arrows) indicative of fibrosis. Panel C: Micro-CT images with three-dimensional reconstructions together with coronal and axial T2-weighted MRI of C57BL/6J mice at 28–30 weeks after whole-thorax irradiation showing increased lung density and decreased lung

volume associated with the presence of pleural effusions. The circle (*) shows a polypropylene tube containing pleural fluid isolated from another irradiated C57BL/6 mouse.

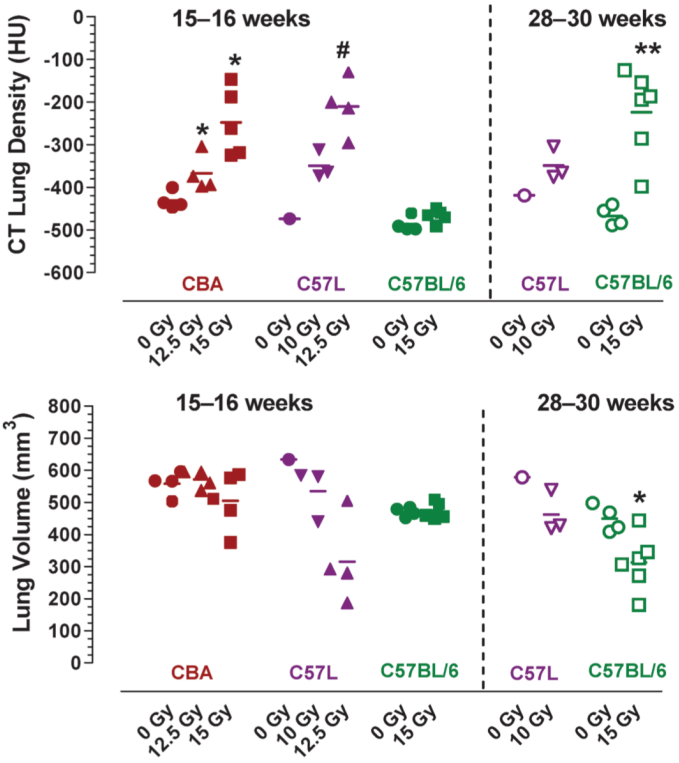

FIG. 4.

Quantitative CT analysis of lung density and volume in individual CBA/J, C57L/J and C57BL/6J mice at 15–16 weeks (closed symbols) or 28–30 weeks (open symbols) after whole-thorax irradiation. * $P < 0.05$, ** $P < 0.01$ compared to unirradiated control of the same strain using Mann-Whitney U test. # $P < 0.05$ for irradiated C57L/J mice compared to CBA/J or C57BL/6J control mice.

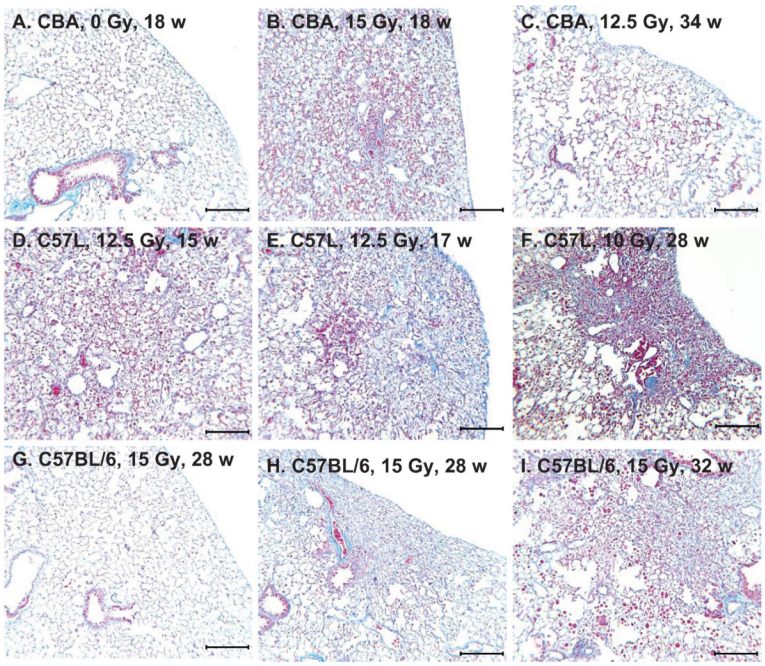

FIG. 5.

Masson's trichrome-stained lung sections from different mouse strains. Panel A: Healthy unirradiated control CBA/J mouse with normal tissue architecture. Lung weight = 211 mg, pleural fluid = 0.02 ml. Panel B: 15 Gy-irradiated CBA/J mouse with respiratory distress at 18 weeks showing severe typical inflammatory pneumonitis (alveolitis) affecting most of the lung tissue. Lung weight = 478 mg, pleural fluid = 0.19 ml. Panel C: 12.5 Gy-irradiated CBA/J mouse with respiratory distress at 34 weeks with pleural effusion showing focal subpleural area of foamy macrophages. Lung weight = 242 mg, pleural fluid = 1.68 ml. Panel D: 12.5 Gy-irradiated C57L/J mouse with respiratory distress at 15 weeks with severe pneumonitis. Lung weight = 563 mg, pleural fluid = 0.04 ml. Panel E: 12.5 Gy-irradiated C57L/J mouse at 17 weeks with respiratory distress with focal collagen deposition surrounded by inflammatory cell infiltrate and edema. Lung weight = 589 mg, pleural fluid = 0.04 ml. Panel F: 10 Gy-irradiated C57L/J mouse without respiratory distress at 28 weeks showing focal contracted fibrosis. Lung weight = 303 mg, pleural fluid = 0.05 ml. Panel G: 15 Gy-irradiated C57BL/6J mouse with respiratory distress at 28 weeks with pleural effusion and mostly normal lung appearance. Lung weight = 254 mg, pleural fluid = 1.26 ml. Panel H: 15 Gy-irradiated C57BL/6J mouse with respiratory distress at 28 weeks with pleural effusion showing focal area of subpleural fibrosis. Lung weight = 286 mg, pleural fluid = 1.02 ml. Panel I: 15 Gy-irradiated C57BL/6J mouse with respiratory distress at 32 weeks with moderate effusion and pneumonitis. Lung weight = 375 mg, pleural fluid = 0.57 ml. Bars represent 250 μm.

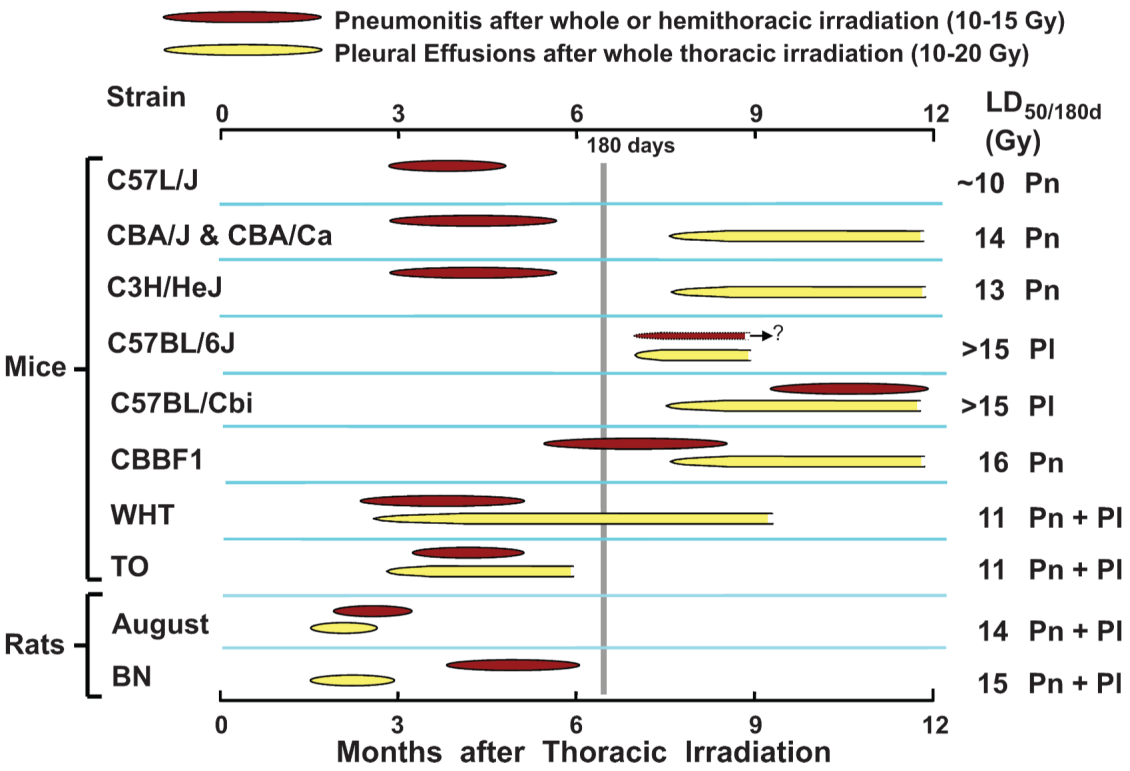

FIG. 6.

The varying development of radiation pneumonitis (Pn) and pleural effusions (Pl) among different rodent strains after thoracic irradiation. The CBA, C57BL/6 and C57L mice from the present studies are compared with CBA/Ca, C57BL/Cbi, their hybrids (CBBF1), WHT, TO and C3H/HeJ mice (12,13) and August (13) and Brown Norway (BN) (15) rats. The late and intermediate development of pneumonitis in C57BL/Cbi and CBBF1 mice, respectively, was seen only after hemithorax irradiation with shielding of the left lung, which prevented pleural effusions (37). C57L, CBA and C3H mice exhibited an early phase attributed exclusively to direct lung damage (pneumonitis) after whole-thorax irradiation with pathology and timing similar to that seen in patients receiving wide-field radiotherapy (3,38).

TABLE 1

Comparison of Different Mouse Strains Irradiated at Two Institutions

Strain	Institution	Radiation source	Dose (Gy)	No. of mice	Survival time (weeks)	Assays
CBA/JIco	UMCG	200 kVp X rays	12.5	5	>40	Breathing rate Gross pathology[c]
CBA/J	MIT	^{137}Cs γ rays	12.5	4	>40	CT imaging Gross pathology Histology
CBA/JIco	UMCG	200 kVp X rays	15.0	5	15.3 ± 1.5[a]	Breathing rate Gross pathology
CBA/J	MIT	^{137}Cs γ rays	15.0	5	18.9 ± 1.0	CT imaging Gross pathology Histology
C57BL/6Ico	UMCG	200 kVp X rays	12.5	5	30.2 ± 3.3	Breathing rate Gross pathology
C57BL/6Ico	UMCG	200 kVp X rays	15.0	5	26.8 ± 1.3	Breathing rate Gross pathology
C57BL/6J	MIT	^{137}Cs γ rays	15.0	7	29.1 ± 1.7	CT imaging Gross pathology Histology
C57L/J	UMCG	200 kVp X rays	10.0	4	17.4 ± 0.4	Breathing rate Gross pathology
	MIT	^{137}Cs γ rays	10.0	3	>28[b]	CT imaging Gross pathology Histology
	UMCG	200 kVp X rays	12.5	5	14.9 ± 0.6	Breathing rate Gross pathology
	MIT	^{137}Cs γ rays	12.5	4	16.3 ± 1.3	CT imaging Gross pathology Histology
	UMCG	200 kVp X rays	15.0	5	16.2 ± 0.8	Breathing rate Gross pathology

[a] Mean ± SD.

[b] C57L/J mice receiving 10 Gy γ rays were euthanized at 28 weeks without respiratory distress.

[c] Gross pathology involved quantification of lung and pleural fluid weights.